# Self-Assembled Nanostructures of Rod−Coil Diblock Copolymers with Different Rod Lengths

**Yingfeng Tu,[†,‡] Xinhua Wan,[†] Hailiang Zhang,[†] Xinhe Fan,[†] Xiaofang Chen,[†] Qi-Feng Zhou,*[,†] and Kinchiu Chau[‡]**

*Department of Polymer Science & Engineering, College of Chemistry and Molecular Engineering, Peking University, Beijing 100871, P. R. China, and Department of Chemistry, The Chinese University of Hong Kong, Shatin, N.T., Hong Kong*

*Received March 18, 2003; Revised Manuscript Received May 29, 2003*

ABSTRACT: Three novel narrowly distributed rod−coil diblock copolymers, poly(styrene-*block*-(2,5-bis-[4-methoxyphenyl]oxycarbonyl)styrene) (PS-*b*-PMPCS), with same PS block length and different PMPCS lengths, were synthesized by 2,2,6,6-tetramethyl-1-piperidinyloxy- (TEMPO-) mediated living free radical polymerization. The self-assembly behavior of the block copolymers in *p*-xylene, which is a good solvent for the PS coils and a selective solvent for the PMPCS rods, was studied by dynamic and static laser light scattering (LLS) and transmission electron microscopy (TEM). The critical association concentration (CAC) for each copolymer was determined and was found to decrease as the molecular weight of the rods increases. We found that the molar mass of the self-assembled nanostructures increased very fast near CAC, while this slows at concentrations much higher than CAC. Dynamic and static LLS revealed that the block copolymers formed core−shell nanostructure in the concentrations we observed, and the radius of the core was calculated. The core−shell nanostructure was also confirmed by TEM images. The calculated radius of the core was compared to the TEM results, and it was found to be compatible.

## Introduction

While distinct polymers are combined together in block copolymers, they can easily self-assemble into a variety of ordered nanostructures in polymer melts[1−5] or in a selective solvent.[5−9] As the former is yet to be fully exploited, the latter, the self-assembly in selective solvents, has attracted much interest. The formation of micelles in a selective solvent is one of the most important and useful properties of block copolymers. Block copolymers are widely used as surfactants, emulsifiers and demulsifiers, stabilizers, and defoamers and are also used in drug delivery systems.[6−9] Because the self-assembly of rod−coil block copolymers is driven by both the selectivity of the solvent and the liquid-crystalline character of the rod blocks, the self-assembly of rod−coil block copolymers in a selective solvent is able to form various of structures with different properties as having been observed experimently[10−13] and predicted by theories.[14−17] Such structures as spherical micelles,[11,18] vesicles,[11] lamellae,[11,19−20] nanoribbons,[21] disklike aggregates,[22] and mushroomlike nanostructures[13] were recently observed. They have made rod−coil block copolymers useful as supramolecular materials and nanomaterials.[11−13,23]

The anionic and cationic polymerizations have been mostly used in synthesizing block copolymers. However, the ionic polymerizations can hardly be applied to the synthesis of rod−coil block copolymers because the ionic initiators may have serious side reactions with the monomers of the rod blocks. The synthesis of rod−coil block copolymers needs careful molecular engineering and forms a challenge to chemists.[10−13,20−26]

During the passed decade, living free radical polymerizations have been a unique technique to prepare macromolecules with controlled architecture[27−30] and have been developed to synthesize liquid crystalline polymers[31−37] and rod−coil block copolymers.[38,39] Recently, we reported a route to synthesize a novel rod−coil block copolymer PS-*b*-PMPCS based on 2,2,6,6-tetramethylpiperidinyl-1-oxy (TEMPO) in combination with benzoyl peroxide (BPO).[38,39] The stiff PMPCS block is a novel mesogen-jacketed liquid crystalline polymer.[38] Since *p*-xylene is a good solvent for PS-*b*-PMPCS at high temperatures (higher than 100 °C) while at room temperatures it is a good solvent for the coil PS but a nonsolvent for PMPCS rods, the block copolymer self-assembles when its *p*-xylene solution is cooled from high temperature to room temperature. From the dynamic and static laser light scattering, we found that the copolymer formed a core−shell nanostructure.[39] By using these two convenient LLS techniques together, we were able to calculate the core radius ($R_c$) and the shell thickness ($\Delta R$) without the need to use the more sophisticated neutron scattering. We revealed that while the average number of the chains assembled in each nanostructure increased with the copolymer concentration, the size of the core remained constant and the PS chains in the shell were stretched and compressed.

The purpose of this work was to study the self-assembly in *p*-xylene of three PS-*b*-PMPCS block copolymers with different lengths of PMPCS by using both dynamic and static laser light scattering in a wide range of polymer concentrations. TEM experiments were carried out to give direct observations of the self-assembly structures and to offer a further support of the core−shell model. The calculated radius of the core from LLS studies was compared to the results from TEM images.

## Experimental Section

**Sample Preparation.** The design and synthesis of the related block copolymers was reported previously.[38,39] Chlorobenzene was used as solvent instead of *p*-xylene in the second step in the preparation for it is a better solvent for

* To whom correspondence should be addressed: E-mail: qfzhou@pku.edu.cn.
[†] Peking University.
[‡] The Chinese University of Hong Kong.

10.1021/ma030178g CCC: $25.00 
Published on Web 07/30/2003

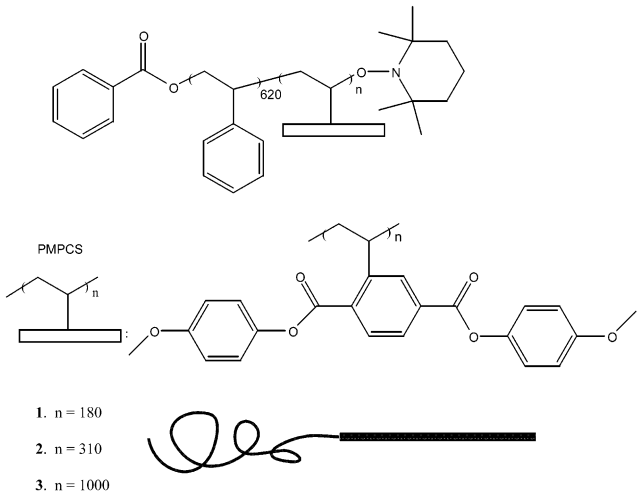


**Figure 1.** Chemical structure and schematic drawing of rod−coil copolymers **1**−**3**.

PMPCS polymers. The number-average molecular weight ($M_n$) and the polydispersity ($M_w/M_n$) were estimated from size exclusion chromatography (SEC, waters 150C) profiles and calibrated with standard PS. The PS-*b*-TEMPO has a number-average molecular weight of 64 600 and a polydispersity index of 1.20 as determined by SEC. The copolymer composition was determined by nuclear magnetic resonance spectroscopy ($^1$H NMR, 400 M Hz) with dichloromethane-$d_2$ as solvent. The block length was estimated from the intensity ratio of the methoxy groups ($\delta$ = 3.3−3.8) and the aromatic groups ($\delta$ = 6.3−7.2). The rod−coil molecule, **1**, and its analogues with longer PMPCS blocks, **2**, and **3**, contained MPCS repeating units of 180, 310, and 1000, with polydispersity indices of 1.24, 1.25, and 1.35, respectively, as presented in Figure 1.

**Laser Light Scattering (LLS).** A slightly modified commercial LLS spectrometer (ALV/DLS/SLS-5022F) equipped with a multi-$\tau$ digital time correlation (ALV5000) and a cylindrical 22 mW uniphase He−Ne laser ($\lambda_0$ = 632 nm) was used. The details of the LLS instrumentation and theory can be found elsewhere.[40,41] In static LLS, the excess absolute time-averaged scattered light intensity, known as the excess Rayleigh ratio $R_{vv}(q)$, of a dilute polymer solution at concentration $C$ (g/mL) is related to the weight-average molar mass $M_w$, the root-mean square $z$-average radius of gyration $\langle R_g^2\rangle_z^{1/2}$ (or written as $\langle R_g\rangle$), and the scattering vector $q$ as the Debye equation

$$\frac{KC}{R_{vv}(q)} \approx \frac{1}{M_w}\left(1 + \frac{1}{3}\langle R_g^2\rangle q^2\right) + 2A_2C \qquad (1)$$

where $K = 4\pi^2n^2(dn/dC)^2/(N_A\lambda_0^4)$ and $q = (4\pi n/\lambda_0)\sin(\theta/2)$ with $N_A$, $dn/dC$, $n$ and $\lambda_0$ being the Avogadro constant, the specific refractive index increment, the solvent refractive index, and the wavelength of the light in a vacuum, respectively, and $A_2$ is the second virial coefficient. The extrapolation of $R_{vv}(q)$ to $q \to 0$ and $C \to 0$ leads to $M_w$. The plots of reduced reciprocal scattered intensity, $[KC/R_{vv}(q)]_{c\to0}$, vs $q^2$ and $[KC/R_{vv}(q)]_{q\to0}$ vs $C$ respectively lead to $\langle R_g^2\rangle$ and $A_2$. For finite concentrations, the so-called Zimm plot of $KC/R_{vv}(q)$ is usually used, which incorporates the extrapolation of $C \to 0$ and $q \to 0$ in a single grid. The specific refractive index increment ($dn/dC$) was determined by a novel and precise differential refractometer.[42] The refractive index increments of PS and PMPCS in *p*-xylene are nearly identical ($dn/dC$ = 0.111 ± 0.002 mL/g for PS and 0.110 ± 0.002 mL/g for PMPCS at 20 °C and 632 nm).

From the plot of $[KC/R_{vv}(q)]_{q\to0}$ vs $C$, the critical association concentration (CAC) of the block copolymer in a selective solvent can be determined. The CAC is located at the concentration where the Debye function departs from its value for unassociated molecules (unimers).[9] To determine the association particle weight near CAC, the solution at the CAC can be considered as the "solvent" for the association particle[43]

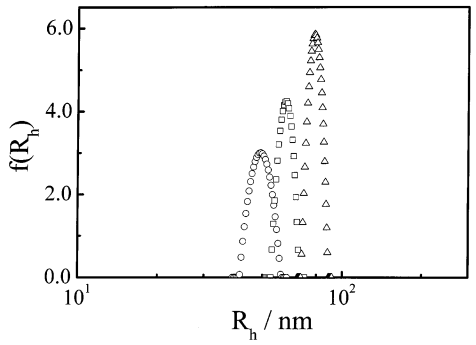


**Figure 2.** Typical hydrodynamic radius of the self-assembled nanostructure of three block copolymers in *p*-xylene at 20 °C: (○) copolymer **1**, 5.0 × $10^{-5}$ g/mL; (□) copolymer **2**, 1.0 × $10^{-5}$ g/mL; (Δ) copolymer **3**, 1.0 × $10^{-5}$ g/mL.

$$\frac{K(C - C_{CAC})}{R - R_{CAC}} \approx \frac{1}{M_w}\left(1 + \frac{1}{3}\langle R_g^2\rangle q^2\right) + 2A_2(C - C_{CAC}) \qquad (2)$$

where $R$ and $R_{CAC}$ are the Rayleigh ratios of the solution and the solution at the CAC, respectively. In this work, the concentration is very dilute and the influence of the $A_2(C - C_{CAC})$ can be neglected. The plot of $K(C - C_{CAC})/(R - R_{CAC})$ vs $q^2$ can thus lead to the apparent molar mass $M_{w,app}$ and $\langle R_g^2\rangle$ of the nanoparticles.

In dynamic LLS,[40] the cumulants analysis of the measured intensity−intensity−time correlation function of a narrowly distributed scattering object could lead to an accurate average line width $\langle\Gamma\rangle$. For a pure diffusive relaxation, $\Gamma$ is related to the translational diffusion coefficient $D$ by $D = (\Gamma/q^2)_{q\to0,C\to0}$ or the hydrodynamic radius $R_h$ by $R_h = k_BT/(6\pi\eta D)$ with $k_B$, $\eta$, and $T$ being the Boltzmann constant, solvent viscosity, and the absolute temperature, respectively.

For block copolymers containing isorefractive copolymer components, the combination of the static and dynamic laser light scattering studies can reveal a lot of characters of the association nanoparticles by using the core−shell model, as we previously described[34]

$$\frac{R_g}{R_h} = \left\{\frac{3[Ax^2 - (1 + A)x^5 + 1]}{5(1 + A)(1 - x^3)}\right\}^{1/2} \qquad (3)$$

where $\langle R_g\rangle$ and $\langle R_h\rangle$ is the $z$-average radius of gyration and hydrodynamic radius of the nanoparticles, $A = M_c/M_s$ is the mass ratio of the core to shell, equals to the mass ratio of the insoluble blocks and soluble blocks, a constant for a given block copolymer, $x = \langle R_c\rangle/\langle R_h\rangle$, is the radius ratio of the core to the outside sphere. Therefore, for each measured $\langle R_g\rangle/\langle R_h\rangle$, we are able to find a corresponding $x$ according to eq 3 and further calculate $\langle R_c\rangle$ and $\langle\Delta R\rangle$ since $\langle R_c\rangle = x\langle R_h\rangle$ and $\Delta R = \langle R_h\rangle - \langle R_c\rangle = \langle R_h\rangle(1 - x)$

**Transmission Electron Microscopy (TEM).** Samples were prepared by directly dropping a corresponding solution onto the carbon coated copper grid and stored for 5 min. The rest of the solution was absorbed by tissue. The samples were then performed on a JEM-100CX II transmission electron microscope and observed directly without any staining.

## Results and Discussion

The size distribution of the hydrodynamic radius from dynamic LLS in Figure 2 shows a clear self-assembly of three kinds of copolymers in *p*-xylene at 20 °C because the hydrodynamic radius in the range 40−150 nm is larger than the individual chains (not more than 20 nm). For all three copolymers, only very narrowly distributed particles were observed, implying they were well-defined, presumably micellelike core−shell nanostruc-

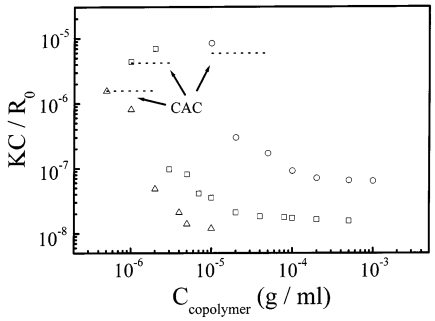


**Figure 3.** Concentration dependence of the reduced scattered intensity of self-assembled nanostructures in *p*-xylene at 20 °C: (○) copolymer **1**; (□) copolymer **2**; (Δ) copolymer **3**. The dashed lines were the ideal reduced scattered intensity for the corresponding individual copolymer. The arrows indicated the CAC of copolymers, where the reduced scattered intensity of the solution decreased abruptly from that of the individual chain.

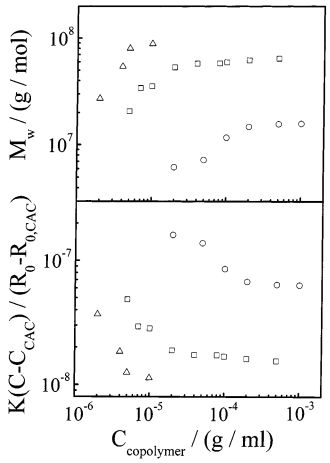


**Figure 4.** Concentration dependence of the adjusted reduced reciprocal scattered intensity (bottom half) and the molar mass (top half) of the self-assembled nanostructures in *p*-xylene at 20 °C: (○) copolymer **1**; (□) copolymer **2**; (Δ) copolymer **3**.

tures, with the insoluble PMPCS as the core and the soluble PS blocks as the shell, as we previously described.[39]

Figure 3 shows the concentration dependence of the reduced reciprocal scattered intensity $(KC/R_{vv(q)})_{q\to 0}$ of three block copolymers in *p*-xylene at 20 °C. It reveals that $(KC/R_{vv(q)})_{q\to 0}$ decreased abruptly when the concentration was higher than a critical concentration. From the onset of change of $(KC/R_{vv(q)})_{q\to 0}$, at where its value equals to corresponding unassociated molecules (individual chain), we can determine the critical association concentration, as pointed in the figure. The results clearly indicate that the CAC decreases when the molecular weight of the rods and the PMPCS blocks increases.

Figure 4 shows that the adjusted reduced reciprocal scattered intensity (calculated by eq 2) decreases as the concentration of the block copolymer increases (Figure 4, bottom half), and thus leads to the increase of the apparent weight-average molar mass of the self-assembly nanoparticles (top half). This is in agreement with our previous report of the PS-*b*-PMPCS block copolymer with different molar masses[39] but is different from the self-assembly of poly(oxyethylene-*block*-oxybutylene) (PEO-*b*-PBO) block copolymers[44] and poly(styrene-*block*-3-hydroxymethylsilacyclobutane) block copolymers,[45] where the averaged molar mass of the

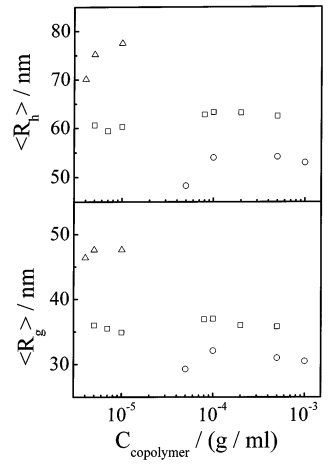


**Figure 5.** Concentration dependence of the hydrodynamic radius ($\langle R_h \rangle$) and the *z*-averaged radius of gyration ($\langle R_g \rangle$) of the self-assembled nanostructures in *p*-xylene at 20 °C: (○) copolymer **1**; (□) copolymer **2**; (Δ) copolymer **3**.

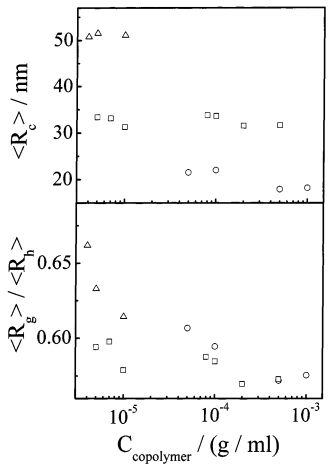


**Figure 6.** Concentration dependence of the ratio of $\langle R_g \rangle/\langle R_h \rangle$ (bottom half) and calculated radius of the core $\langle R_c \rangle$ (top half) of the self-assembled nanostructures in *p*-xylene at 20 °C: (○) copolymer **1**; (□) copolymer **2**; (Δ) copolymer **3**.

assembled particles does not change as the concentration changes. At concentrations near CAC, $M_{w,app}$ increases very fast when the concentration increases, meaning a fast increase of the number of the copolymer chains which are assembled into the nanostructures. However, at concentrations much higher than CAC, $M_{w,app}$ increases slowly and tends to reach a plateau. This should be due to the repulsion of the soluble PS blocks in the shell, which tend to take more space in a good solvent and prevent insertion of more chains into the already densely packed core. For copolymer **3**, which has the highest molar mass, at concentrations of $2.0 \times 10^{-5}$ g/mL and higher, the scattered intensity reduced a lot after filtration, which meant that there existed large particles in the solution, and thus it could not be studied by LLS at those concentrations.

The *z*-averaged radius of gyration $\langle R_g \rangle$ and the hydrodynamic radius $\langle R_h \rangle$ of the nanoparticle increase slowly when the concentration increases, as shown in Figure 5. The ratio of $\langle R_g \rangle/\langle R_h \rangle$ for copolymers **1**, **2**, and **3** (at concentrations below $2.0 \times 10^{-5}$ g/mL) was calculated and found to decrease as the concentration increased, as presented in the lower part of Figure 6. The calculated ratios of $\langle R_g \rangle/\langle R_h \rangle$ for the three copolymers are around 0.6, all much lower than the value

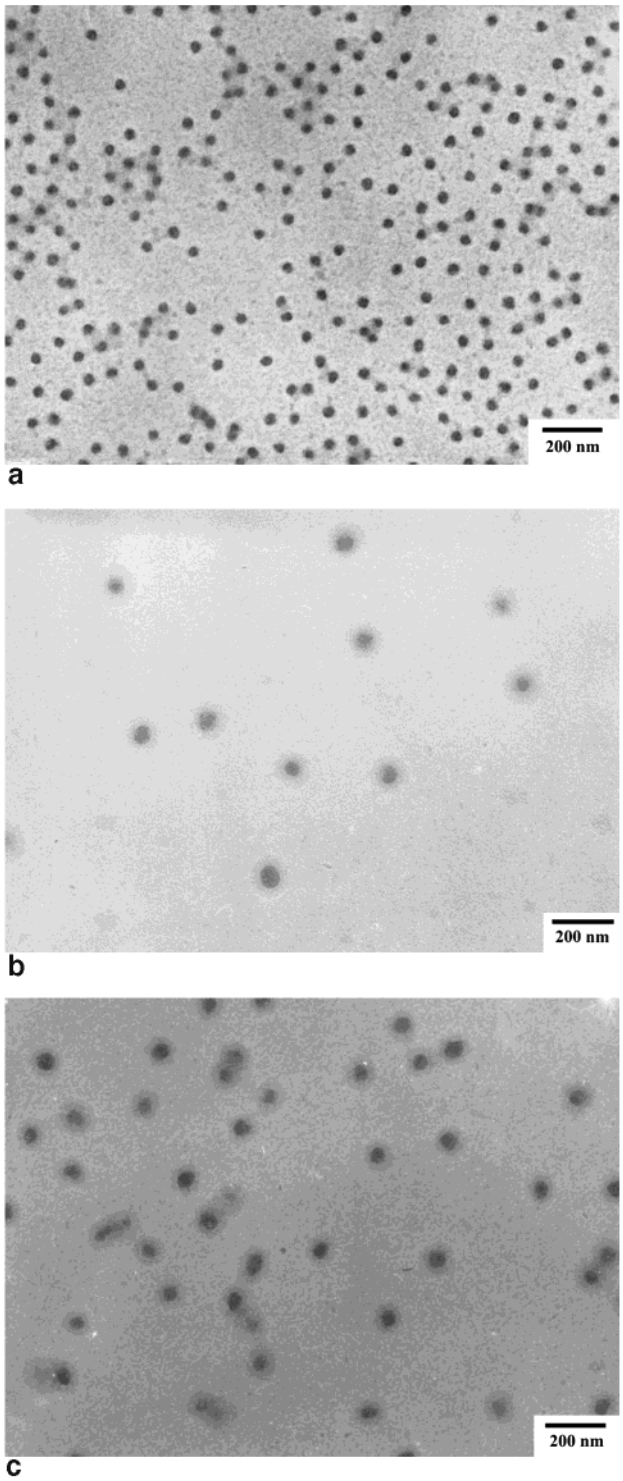


**Figure 7.** TEM images of the self-assembled nanostructures of copolymer **1** and **2** in *p*-xylene**.** Samples were observed directly without any staining. Key: (a) copolymer **1**, $2.0 \times 10^{-3}$ g/mL; (b) copolymer **2**, $1.0 \times 10^{-4}$ g/mL; (c) copolymer **2**, $5.0 \times 10^{-4}$ g/mL.

0.775 for uniform spheres but close to our previously reported value for a similar block copolymer, indicating that the nanostructures of these copolymers can also be described with the core−shell model.[39] Similar low values of $\langle R_g \rangle / \langle R_h \rangle$ were also observed in polystyrene microgels,[46] block copolymer particles,[47] and block ionomer micelles[48] and for the adsorption of polymer chains on colloid particles.[49] The radii $\langle R_c \rangle$ of the cores of the nanostructures were calculated from eq 3, by using the values of $\langle R_g \rangle / \langle R_h \rangle$, and are presented in the upper part of Figure 6. For copolymers **1**, **2**, and **3**, $\langle R_c \rangle$ remained almost the same for a given copolymer, but increased as the molecular weight of the PMPCS increased; i.e., $\langle R_c \rangle$ increased when the rod became longer.

Figure 7a is a typical TEM image of copolymer **1** at a concentration of $2.0 \times 10^{-3}$ g/mL, while parts b and c of Figure 7 are of the copolymer **2** at $1.0 \times 10^{-4}$ g/mL and $5.0 \times 10^{-4}$ g/mL respectively. The figures show only individual spherical micelles and prove the core−shell model. The dark cores of the spheres should be attributed to the PMPCS rods because the rods contain heavier atoms (oxygen) than PS coils and scatter electrons more strongly than PS coils. Conversely, the gray regions around the dark cores should be attributed to PS coils. In Figure 7a, the radii of the cores observed by TEM images are 18−20 nm. In parts b and c of Figure 7, they are 25−30 nm. The results coincide well with, though a little smaller than, that from LLS studies which gave the value of about 20 nm for copolymer **1** and 31 nm for copolymer **2**. The somewhat lower value from TEM than from LLS may be attributed to the shrinking of the cores during the solvent evaporation in the preparation of the TEM samples, and may also be due to the fact that light scattering yields the *z*-average radius of gyration, which is very sensitive to the presence of even small amounts of large particles.

## Conclusions

Three rod−coil diblock copolymers PS−PMPCS with same PS length but different PMPCS length were synthesized. The self-assembly of the copolymers in *p*-xylene was studied by static and dynamic laser light scattering. The CAC of the copolymers was found to decrease when the molecular weight of the PMPCS increased. The molar mass of the self-assembled nanoparticles increased very fast as the concentration increased around CAC but remained almost unchanged at much higher concentrations, where the nanoparticles became densely packed and the repulsions between the soluble PS blocks prevented more chains from inserting into the nanoparticles. By a combination of static and dynamic LLS, we found that these copolymers could form core−shell nanostructures at the concentration we studied. The radius of the cores of each copolymer remained unchanged as the concentration increased. The core−shell model of the self-assembled nanostructures was supported by TEM studies and the radii obtained from LLS and TEM agreed well with each other.

**Acknowledgment.** We greatly thank Prof. Chi Wu at The Chinese University of Hong Kong for his advice and helps. The financial support of National Natural Science Foundation of China (NNSFC), Grants 29992590-4 and 20134010, is gratefully acknowledged.

## References and Notes

(1) Bates, F. S.; Fredrickson, G. H. *Ann. Rev. Phys. Chem.* **1990**, *41*, 525.
(2) Fredrickson, G. H.; Bates, F. S. *Ann. Rev. Mater. Sci.* **1996**, *26*, 501.
(3) Colby, R. H. *Curr. Opin. Colloid Interface Sci.* **1996**, *1*, 454.
(4) Ryan, A. J.; Hamley, I. W. Morphology of Block Copolymers. In *The Physics of Glassy Polymers*; Haward, R. N., Yang, R. J., Eds.; Chapman and Hall Press: London, 1997.
(5) Hamley, I. W. *The Physics of Block Copolymers*; Oxford University Press: Oxford, England, 1998.

(6) Booth, C.; Price, C. *Comprehensive Polymer Science*; Pergamon Press: Oxford, England, 1989.
(7) Tuzar, Z.; Kratochvíl, P. Micelles of block and graft copolymers in solutions. In *Surface and Colloid Science*; Matijevic, E., Ed.; Plenum Press: New York, 1993; Vol. 15.
(8) Chu, B. *Langmuir* **1995**, *11*, 414.
(9) Alexandridis, P.; Lindman, B. *Amphiphilic Block Copolymers: Self-Assembly and Applications*; Elsevier: Amsterdam, 2000.
(10) Chen, J. T.; Thomas, E. L.; Ober, C. K.; Mao, G. P. *Science* **1996**, *273*, 343.
(11) Jenekhe, S. A.; Chen, X. L. *Science* **1998**, *279*, 1903.
(12) Cornelissen, J. J. L. M.; Fischer, M.; Sommerdijk, N. A. J. M.; Nolte, R. J. M. *Science* **1998**, *280*, 1427.
(13) Stupp, S. I.; LeBonheur, V.; Walker, K.; Li, L. S.; Huggins, K. E.; Keser, M.; Amstutz, A. *Science* **1997**, *276*, 384.
(14) Halperin, A. *Macromolecules* **1990**, *23*, 2724.
(15) Semenov, A. N. *Mol. Cryst. Liq. Cryst.* **1991**, *209*, 191.
(16) Williams, D. R. M.; Fredrickson, G. H. *Macromolecules* **1992**, *25*, 3561.
(17) Matsen, M. W.; Barrett, C. *J. Chem. Phys.* **1998**, *109*, 4108.
(18) Wu, C.; Niu, A.; Leung, L. M.; Lam, T. S. *J. Am. Chem. Soc.* **1999**, *121*, 1954.
(19) Klok, H. A.; Langenwalter, J. F.; Lecommandous, S. *Macromolecules* **2000**, *33*, 7819.
(20) Ohtake, T.; Takamitsu, Y.; Akita, K. I.; Kanie, K.; Yoshizawa, M.; Mukai, T.; Ohno, H.; Kato, T. *Macromolecules* **2000**, *33*, 8109.
(21) Zubarev, E. R.; Pralle, M. U.; Li, L.; Stupp, S. I. *Science* **1999**, *283*, 523.
(22) Wu, J.; Pearce, E. M.; Kwei, K. T.; Lefebvre, A. A.; Balsara, N. P. *Macromolecules* **2002**, *35*, 1791.
(23) Alivisatos, A. P.; Barbara, P. F.; Castleman, A. W.; Chang, J.; Dixon, D. A.; Klein, M. L.; McLendon, G. L.; Miller, J. S.; Ratner, M. A.; Rossky, P. J.; Stupp, S. I.; Thompson, M. E. *Adv. Mater.* **1998**, *10*, 1297.
(24) Yamada, M.; Itoh, T.; Nakagawa, R.; Hirao, A.; Nakahama, S.; Watanabe, J. *Macromolecules* **1999**, *32*, 282.
(25) Lee M.; Cho, B.-K.; Kang, Y.-S.; Zin, W.-C. *Macromolecules* **1999**, *32*, 7688.
(26) Schneider, A.; Zanna, J.-J.; Yamada, M.; Finkelmann, H.; Thomann, R. *Macromolecules* **2000**, *33*, 649.
(27) Georges, M. K.; Veregin, R. P. N.; Kazmaier, P. M.; Hamer, G. K. *Macromolecules* **1993**, *26*, 2987.
(28) Hawker, C. J. *J. Am. Chem. Soc.* **1994**, *116*, 11185.
(29) Wang, J. S.; Matyjaszewski, K. *J. Am. Chem. Soc.* **1995**, *117*, 5614.
(30) Kato, M.; Kamigato, M.; Sawamoto, M.; Higashimura, T. *Macromolecules* **1995**, *28*, 1721.
(31) Wan, X.-h.; Tu, H.-l.; Tu, Y.-f.; Zhang, D.; Sun, L.; Zhou, Q.-f. *Chin. J. Polym. Sci.* **1999**, *17*, 189.
(32) Pragliola, S.; Ober, C. K.; Mather, P. T.; Jeon, H. G. *Macromol. Chem. Phys.* **1999**, *200*, 2338.
(33) Chang, C.; Pugh, C. *Macromolecules* **2001**, *34*, 2027.
(34) Gopalan, P.; Ober, C. K. *Macromolecules* **2001**, *34*, 5120.
(35) Kasko, A. M.; Grunwald, S. R.; Pugh, C. *Macromolecules* **2002**, *35*, 5466.
(36) Gopalan, P.; Andruzzi, L.; Li, X. F.; Ober, C. K. *Macromol. Chem. Phys.* **2002**, *203*, 1573.
(37) Zhang, H.; Yu, Z.; Wan, X.; Zhou, Q.-F.; Woo, E. M. *Polymer* **2002**, *43*, 2357.
(38) Wan, X.; Tu, Y.; Zhang, D.; Zhou, Q.-F *Polym. Int.* **2000**, *49*, 243.
(39) Tu, Y.; Wan, X.; Zhang, D.; Zhou, Q.-F.; Wu, C. *J. Am. Chem. Soc.* **2000**, *122*, 10201.
(40) Berne, B. J.; Pecora, R. *Dynamic Light Scattering*; Plenum Press: New York, 1976.
(41) Chu, B. *Laser Light Scattering*, 2nd ed.; Academic Press: New York, 1991.
(42) Wu, C.; Xia, K.-Q. *Rev. Sci. Instrum.* **1994**, *65*, 587.
(43) Debye, P. *J. Colloid Sci.* **1948**, *3*, 407.
(44) Yang, Y.-W.; Deng, N.-J.; Yu, G.-E.; Zhou, Z.-K.; Attwood, D.; Booth, C. *Langmuir* **1995**, *11*, 4703.
(45) Matsumoto, K.; Miyagawa, K.; Matsuoka, H.; Yamaoka, H. *Polym. J.* **1999**, *31*, 609.
(46) Antonietti, M.; Bremser, W. *Macromolecules* **1990**, *23*, 3796.
(47) Tauer, K.; Khrenov, V. *Macromol. Symp.* **2002**, *179*, 27.
(48) Moffitt, M.; Yu, Y.; Nguyen, D.; Graziano, V.; Schneider, D. K.; Eisenberg, A. *Macromolecules* **1998**, *31*, 2190.
(49) Wu, C.; Gao, J. *Macromolecules* **1999**, *32*, 1704.

MA030178G